CHANNEL MODELLING & PERFORMANCE ANALYSIS OF WIFI

Jivisha, Gaurav Mohta, Saumya Das

Sikkim Manipal Institute of Technology

Email Id- gauravmohta.official@gmail.com; Ph No. +91 9609850304

Abstract— Wi-Fi or wireless fidelity is a wireless way to handle networking. It is also known as 802.11 networking. In this paper we have proposed the technique of channel modelling using a modified Saleh-Valenzuela model, using Nakagami-m distribution of small scale fading. The modelling is done for the following frequency ranges: for UWB channels covering frequency range from 2 to 10 GHz. This range covers indoor residential, indoor office, industrial, outdoor and open outdoor environments with a contrast between LOS and NLOS properties. Through this paper 100 impulse responses are realized for each environment.

Keywords— channel modeling, Complementary Code keying(CCK), Saleh-Valenzuela, Nakagami-m distribution, Ultra Wide Band (UWB) channels, Orthogonal Frequency Division Multiplexing (OFDM) channels, Line of Sight (LOS), Non-Line of Site (NLOS)

INTRODUCTION

Wi-Fi or wireless fidelity is a wireless way to handle networking. It is also known as 802.11 networking. Using this technology we can connect computers anywhere in a home or office without using wires. An average speed of 54 Mbps is provided. In 1999 IEEE 802.11b was introduced. 802.11b defines the physical layer and media access control (MAC) sub layer for communication across a shared WLAN. At physical layer, 802.11b operates at 2.45 GHz with maximum bit rate of 11 Mbps. At MAC sub layer, 802.11b uses carrier sense multiple access with collision avoidance (CSMA/CA) protocol. For IEEE 802.11g standard uses 2.4GHz and provides a data rate of 54 Mbps. It specifies OFDM and CCK modulation schemes with 24Mbps as maximum mandatory data rate[3]. The disadvantages observed in 802.11b and 802.11g are that they use 2.4 GHz spectrum which is crowded with other devices such as Bluetooth, microwave ovens, cordless phones, or video sender devices, among many others. This may cause degradation in performance. Also Power consumption is fairly high compared to other standards, making battery life and heat a concern. With the aim of providing "Very High Throughput" (VHT) IEEE 802.11 ad was introduced in the year 2003. Wi-Fi ad or WiGig defines a new physical layer operating at 60 GHz wave spectrum [3]. The bandwidth allocation is between 2.4 GHz – 5 GHz. 60 GHz wave transmissions will scale the speed of WLANs and WPANs to 6.75 Gbits/s over a distance of 10 meters. It supports FST (Fast Session Transfer) protocol which makes it backward compatible with 5 GHz or 2.4 GHz[4]. For making 802.11 ad compatible at the Medium Access Control (MAC) or Data Link Layer , devices consists of three radios: 2.4 GHz for general use which may suffer from interferences, 5 GHz for more robust and higher speed applications , and 60 GHz for ultra-high-speed within a room. It also supports session switching between the 2.4GHZ, 5GHz and 60 GHZ unlicensed band. The MAC protocol is based on TDMA and Physical layer uses SC (Single Carrier) and OFDM (Orthogonal Frequency Division Multiplexing) to simultaneously enable low power, high-performance applications [3].

In previous researches, the concept of large scale fading, small scale fading (Rayleigh fading) has been proposed. Large scale fading between the transmitter and receiver is predominantly affected by large hills, forests, buildings etc. Small scale fading refers to change in signal amplitude and phase that is experienced as a result of small changes in between the transmitter and receiver. Small scale fading is dependent on two factors, namely, time spreading of signal (signal dispersion) and time variant behavior of channel. For mobile applications, the channel is time variant because of the motion between transmitter and receiver results in change in propagation paths. The rate of change of these propagation conditions is called 'fading rapidity'. Small-scale fading is also called Rayleigh fading because if the multiple reflective paths are large in number and there is no line-of-sight (LOS) signal component, the envelope of the received signal is statistically described by a Rayleigh PDF. There are three basic factors that affect signal propagation in systems. They are reflection, diffraction and scattering. [2]

1. Reflection occurs when a propagating electromagnetic wave impinges on a smooth surface with very large dimensions compared to the RF signal wavelength (λ).
2. Diffraction occurs when the radio path between the transmitter and receiver is obstructed by a dense body with large dimensions compared to ' λ '. Diffraction is a phenomenon that accounts for RF energy travelling from transmitter to receiver without a line of-sight path between the two. It is often termed shadowing because the diffracted field can reach the receiver even when shadowed by an impenetrable obstruction.
3. Scattering occurs when a radio wave impinges on either a large rough surface or any surface whose dimensions are in the order of λ or less, causing the reflected energy to spread out (scatter) in all directions.

Ultra Wide Band (UWB) channels tends to push the limit of bandwidth to about 500 MHz or more or uses a bandwidth that is 20% or larger than the carrier frequency. We use UWB channel in this paper because of the property of UWB channels i.e. impulse responses of UWB can be 'sparse' i.e. characterized by a few spikes separated by time during which no significant energy arrives. The

fundamental mechanism of wireless communication is multipath propagation. The electromagnetic fields sent from transmitted antenna are components of magnetic fields transmitted in different directions [2]. Each of the components now propagates in space and might be reflected, diffracted, or scattered by objects (mountains, houses, trees, walls, furniture) in the environment, (see Fig.1)
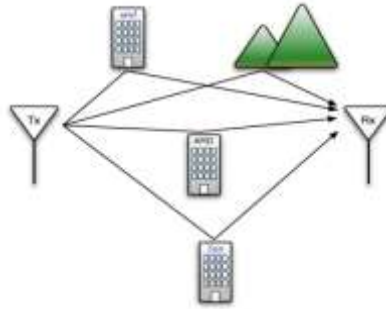

Fig.1
MULTI PATH TRANSMISSION

Each interaction process can change the direction of the components, and some interactions (like diffraction) might even split up the components into multiple new components. This causes multipath components.

For this paper, we have designed a modified Saleh-Valenzuela model, consisting of Nakagami-m distribution of small scale fading, with different m-factors for different components [3].

MODELLING

According to the recommendations of channel modelling subgroup of IEEE 802.15.4a, the task group has to mandate an alternative physical layer for sensor networks and similar devices working with the IEEE 802.15.4a MAC layer. The main goal of the proposal was to develop an energy efficient data communication with data rates between 1Kbps and several MegaKBps and with the capability of geo-locations. With the channel modelling, we try to make a fair comparison of different proposals. The main goals of the model described in the document are the modelling attenuation and delay dispersion. Modelling of attenuation includes shadowing and average path loss and in delay dispersion power delay profile and small scale fading statistics are included. From these other parameters such as rms delay spread, number of multipath components carrying x% of the energy etc. are being considered [3].

The generic model described for different frequency ranges are almost similar but the parameterizations are different. All the models discussed are time continuous and the impulse responses are being generated with the help of MATLAB program and its being tested for different underlying environments.

We derived number of environments discussed for the evaluation of the model. The list discussed is not comprehensive and cannot cover all possible future applications [1]:

   i.   Indoor residential: Environment for home networking. Buildings consist of small units with walls of reasonable thickness.
   ii. Indoor office: Due to partitioning of unit, higher attenuation is given by furniture, cubicles, labs etc.
   iii. Industrial environments: These are characterized by larger enclosures (factory halls), filled with a large number of metallic reflectors .This is anticipated to lead to severe multipath.
   iv. Body-area network (BAN): It is characterized by the wireless network of wearable computing devices. Channel model for this is considered to be very different for this environment as the main scattering is in the near field region of the antenna.
   v.   Outdoor: While a large number of different outdoor scenarios exist, the current model covers only a suburban-like microcell scenario, with a rather small range.
   vi. Agricultural areas/farms: For those areas, few propagation obstacles (silos, animal pens), with large distances in between, are present. Delay spread can thus be anticipated to be smaller than in other environments.

The key features for the generic channel model are summarized below before going into details [1]

   • model treats only channel, while antenna effects are to be modeled separately
   • d−n law for the pathloss
   • frequency dependence of the pathloss
   • modified Saleh-Valenzuela model:
       – Arrival of paths in clusters.
       – Mixed Poisson distribution for ray arrival times.
       – Possible delay dependence of cluster decay times.
       – some NLOS environments first increase, then decrease of power delay profile referring
   • Nakagami-distribution of small-scale fading, with different m-factors for different components
   • Block fading: Channel stays constant over data burst duration.

SALEH VALENZUELA MODEL - It is described as a statistical model where it is assumed that multipath components (MPCs) arrive in clusters which are formed by the multipath reflections from various components placed in the vicinity of transmitter and receiver. Different arrival rate of clusters in the MPCs as well as inter cluster arrival rates are described with the help of Poisson Processes that are exponentially distributed.

The complex, impulse response described for this channel in general is given by:-

$$h(t) = \sum_{l=0}^{\infty} \sum_{k=0}^{\infty} \beta_{kl} e^{j\theta kl} \delta(t - T_l - \tau_{kl}) \tag{1}$$

Where, T_l is the arrival time of lth cluster and τ_{kl} is the the arrival time of the kth ray measured from the beginning of the lth cluster, while β_{kl} is the gain of the kth ray of the lth cluster. The phases θ_{kl} are uniformly distributed i.e., for a bandpass system, the phase is taken as a uniformly distributed random variable from the range $[0, 2\pi]$.

As we have earlier mentioned that number of clusters L in MPCs is assumed to be a Poisson distributed process which can be formulated by given equation:-

$$PDF_l(L) = \frac{(\bar{L})^L e^{(-\bar{L})}}{L!} \tag{2}$$

Where, L and $\bar{L}$ completely characterizes the distribution.

Within each clusters, Cluster arrivals are Poisson distributed with rate ʌ (cluster arrival rate) and ray arrival rates in the cluster are also Poisson distributes with rate λ (ray arrival rate) such that,   λ >> ʌ. The definition assumes that within a cluster, the first ray arrives with no delay ($\tau_{0,l} = 0$). The distribution of cluster arrival time with the ray arrival time is described by given equations:-

$$p(T_l/T_{l-1}) = \Lambda exp[-\Lambda(T_l - T_{l-1})], l > 0 \tag{3}$$

$$p(\tau_{k,l}/\tau_{(k-1),l}) = \lambda \exp[-\lambda(\tau_{k,l} - \tau_{(k-1),l})], k > 0 \tag{4}$$

In this document to accord the variation in the fitting for the indoor residential, and indoor and outdoor environments, we model the ray arrival times as the mixtures of two Poisson processes as follows:-

$$p(\tau_{k,l}/\tau_{(k-1),l}) = \beta\lambda_1 exp[-\lambda_1(\tau_{k,l} - \tau_{(k-1),l})] + (\beta - 1)\lambda_2 exp[-\lambda_2(\tau_{k,l} - \tau_{(k-1),l})], k > 0 \tag{5}$$

Where β - is the mixture probability of two successive rays in the cluster and λ_1, λ_2 are the ray arrival rates

Now while discussing about the different environments through which all the RF signals pass, we can see that the radio signals are being reflected from tall buildings, walls, furniture and other conducting surfaces. We define different clusters of different shapes and sizes for these incoming signals arriving at receiver at different times with different amplitude from different directions after multiple reflections. According to Saleh Valenzuela model the Power Delay Profile for our model, was observed as the subsequent clusters which were further attenuated in amplitude and also arrivals within a single cluster decayed with time. These decaying patterns are exponential within each cluster which can be represented as:-

$$E\{|b_{k,l}|^2\} = \Omega_l \frac{1}{\gamma_l[(1-\beta)\lambda_1 + \beta\lambda_2 + 1]} \exp(-\tau_{k,l}/\gamma_l) \tag{6}$$

Where Ω_l is the integrated energy constant and λ_l is the inter- cluster decay time constant of the l_{th} cluster. Whereas it has been seen that the shape of the power delay profile can be different for the NLOS case of different environments so we can use this modified form:-

$$E\{|b_{k,l}|^2\} = (1 - \chi.\exp(-\tau_{k,l}/\gamma_{rise})).\exp(-\tau_{k,l}/\gamma_1).\frac{\gamma_1 + \gamma_{rise}}{\gamma_1}\frac{\Omega_1}{\gamma_1 + \gamma_{rise}(1 - \chi)} \tag{7}$$

Here, the parameter χ describes the attenuation of the first component, the parameter γ_{rise} determines how fast the PDP increases to its local maximum, and γ_1 determines the decay at late times.

The cluster decay time is linearly dependent on the arrival time of the cluster, described as:-

$$\gamma_l \propto j_\gamma T_l + \gamma_0 \tag{8}$$

Where j_γ describes the increase of the decay constant with the delay.

The above parameters give a complete description of the Power Delay Profile of our model. Apart from these parameters we will be using some of the auxiliary parameters for the better comparison with the existing measurements

RMS delay spread and mean excess delay are multipath channel parameters that can be determined from a Power Delay Profile. The mean excess delay is the first moment of the power delay profile and it is described as:

$$\bar{\tau} = \frac{\sum_k p(\tau_k)\tau_k}{\sum_k p(\tau_k)} \tag{9}$$

Where $p(\tau_k)$ is the power measured at the time τ of the k_{th} ray arrival.

The rms delay spread is the root mean square of the second moment of the power delay profile and is defined to be:

$$\sigma_\tau = \sqrt{\overline{\tau^2} - \left(\bar{\tau}\right)^2} \tag{10}$$

Where,

$$\overline{\tau^2} = \frac{\sum_k p(\tau_k)\tau_k^2}{\sum_k p(\tau_k)}$$

Another auxiliary parameter such as the number of multipath components that is within x dB of the peak amplitude, or the number of MPCs that carries at least y % of the total energy. These are determined from the power delay profile with the amplitude fading statistics.

Nakagami-m distribution is the generalized distribution which can model different fading environments. It has much greater flexibility and accuracy than Rayleigh, Rician or logarithmic distributions. The following small scale fading pdf is Nakagami:

$$pdf(x) = \frac{2}{\Gamma(m)}\left(\frac{m}{\Omega}\right)x^{2m-1}\exp\left(-\frac{m}{\Omega}x^2\right) \tag{11}$$

Where $m \geq 1/2$ is the Nakagami-m factor, $\Gamma(m)$ is the gamma function, Ω is the mean-square value of amplitude.

RESULTS

Depending on the mathematical model of Saleh- Valenzuela model and Nakagami-m small scale fading we generate MATLAB code for the channel model condition. We characterized the environments in 8 different channel conditions. These channel conditions includes all different environmental conditions and frequency ranges. These conditions are basically those environments which are common for signal transfer nowadays.

We generated 100 impulse responses for the testing of our mathematical channel modeling. Each of these impulse responses were normalized to unit energy. These impulse responses were tested in all the environmental conditions specified. Depending on the results observed we have displayed a tabular comparative study of all the channel conditions as follows:-

CHANNEL NO.	CHANNEL CONDITION	MEAN DELAY(Ns)	RMS DELAY(Ns)	Number of paths within 10 dB	Number of paths capturing >85% energy
1	Residential LOS	16.0	17	15.3	54.6
2	Residential NLOS	19.9	19	35.6	110.7
3	Office LOS	9.6	10	14.3	22.3
4	Office NLOS	18.4	13	30.4	45.3
5	Outdoor LOS	26.8	30	17.9	35.9
6	Outdoor NLOS	72.8	74	24.7	65
7	Industrial LOS	1.6	9	6.7	8.7
8	Industrial NLOS	23.9	20	128.5	186.6

Table No. 1

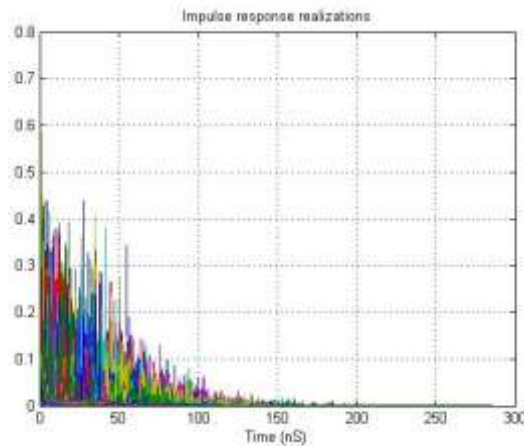## CHANNEL NO. 1- RESIDENTIAL LOS

Fig. 2- Impulse response realizations

This graph displays the variation of 100 impulses with time. Different colours in graph denote different impulse realizations. We can clearly infer from the graph, that impulse strength is higher in the time period between 0 to 50 (nS). Signal strength decays as the time increases and completely fades away after 200 (nS).
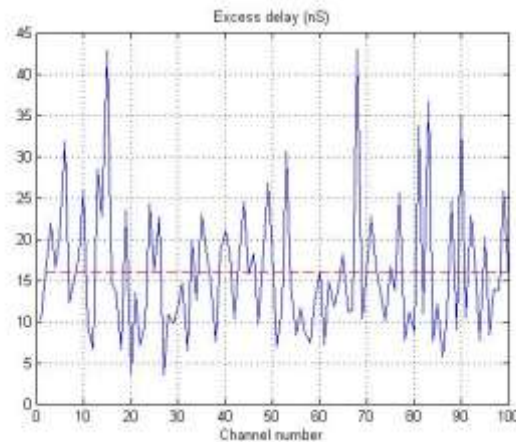

Fig.2- Excess delay

This graph is for the realization of excess delay with the different channel number responses. We can see from the graph that 68th impulse response have the highest excess delay of 42.98 (nS) and 27th impulse response have the lowest excess delay of 3.51(nS). The red margin is set at the minimum excess delay required for our channel model which is at 15.98 (nS).
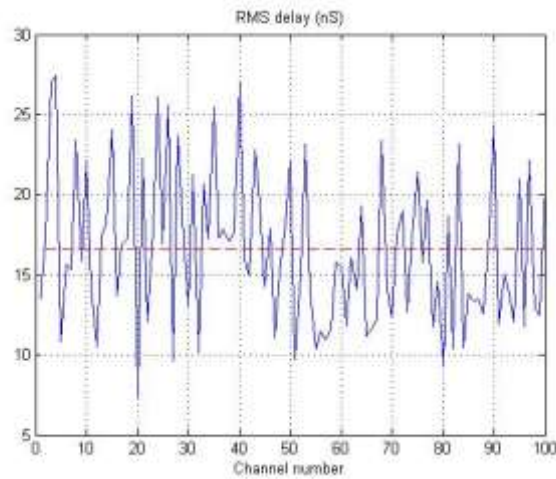

Fig.3- RMS delay

This graph is for the realization of RMS delay with the different channel number responses. We can see from the graph that 4th impulse response have the highest RMS delay of 27.42 (nS) and 20th impulse response have the lowest RMS delay of 7.377 (nS). The margin at 16.57 (nS) is set according to the minimum required RMS delay for the model.
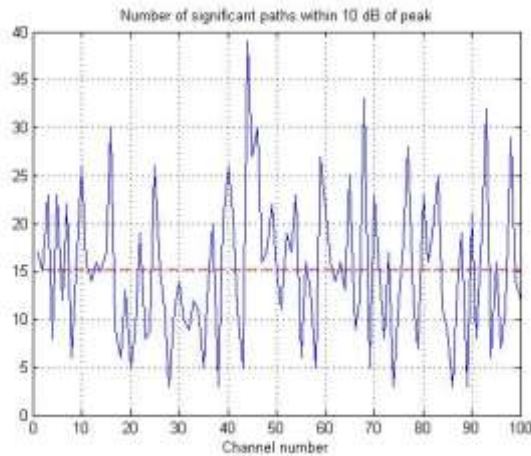

Fig.4- Number of significant paths within 10 dB of peak

Threshold energy for the channel is set at -10 or 10 dB. We tried to find out the number of significant multipath components whose energy is greater than 10 dB peak. We compared the absolute value of 1st column of our obtained matrix with the threshold energy of all the impulse responses. For channel no 1 total no of significant multipath components are found to be 15.3.
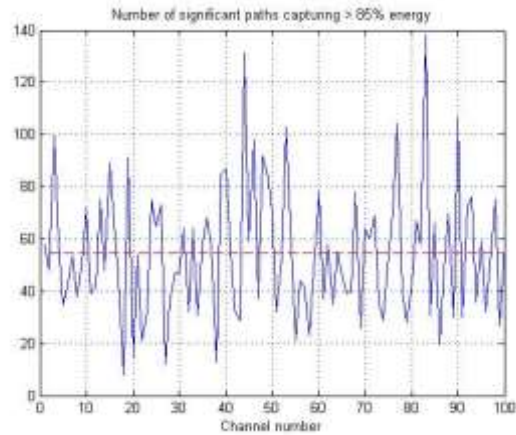
Fig.5- Number f significant paths capturing > 85% energy

To determine the number of significant paths capturing 85% of energy in channel, we compared the cumulative energy of all the received impulse responses with the sorted cumulative sum of energy of the individual impulses matrices. For channel number 1 no. Of significant paths are 54.6.
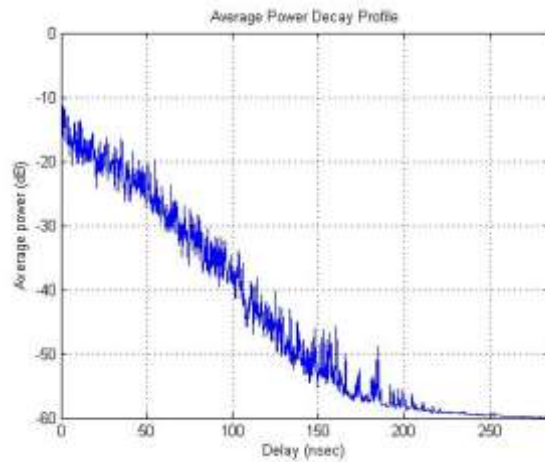

Fig.6- Average Power Decay Profile

Power decay profile is exponentially within each cluster which can be easily demonstrated with the observed graph. We have plotted our graph between the average decay profile in (dB) which is greater than the threshold level of -40. Average power is highest within the range of 0-50(nS) and then it decays eventually as delay increases.

CONCLUSION

Through this paper we have tried to model the modified Saleh- Valenzuela model for the UWB channel. In this paper the model describes the channel only excluding the antenna effects. We have tested the designed channel in different environmental conditions both in LOS and NLOS regions. The data sheet specified above gives the value of different parameter values of these channel conditions. We have discussed the graph observed for the channel no. 1 i.e. residential LOS in our results. The future scope of our project will be the implementation of our channel in our practical Wi-Fi-ad system. The BER, PER and throughput of Wi-Fi system would increase using this channel model.

REFERENCES:

[1] Molisch, A.F.; Cassioli, D.; Chia-Chin Chong; Emami, S.; Fort, A.; Kannan, B.; Karedal, J.; Kunisch, J.; Schantz, H.G.; Siwiak, K.; Win, M.Z., "A Comprehensive Standardized Model for Ultrawideband Propagation Channels," *Antennas and Propagation, IEEE Transactions on* , vol.54, no.11, pp.3151,3166, Nov. 2006

[2] Molisch, A.F., "Ultra-Wide-Band Propagation Channels," *Proceedings of the IEEE* , vol.97, no.2, pp.353,371, Feb. 2009

[3] Daniels, R.C.; Murdock, J.N.; Rappaport, T.S.; Heath, R.W., "60 GHz Wireless: Up Close and Personal," *Microwave Magazine, IEEE* , vol.11, no.7, pp.44,50, Dec. 2010

[4] Perahia, E.; Cordeiro, Carlos; Minyoung Park; Yang, L.L., "IEEE 802.11ad: Defining the Next Generation Multi-Gbps Wi-Fi," *Consumer Communications and Networking Conference (CCNC), 2010 7th IEEE* , vol., no., pp.1,5, 9-12 Jan. 2010

[5] Mishra, Mukesh K.; Sood,Netu; Sharma, Ajay K., "Efficient BER Analysis of OFDM System over Nakagami-m Fading Channel," *International Journal of Advanced Science and Technology, Vol. 37, Dec. 2011.*
[6] Chunlei Yin; Guangjun Wen; Zhengyong Feng, "Simulation research of 802.11n channel model D in NS2," *Computer Science and Information Technology (ICCSIT), 2010 3rd IEEE International Conference on* , vol.7, no., pp.530,533, 9-11 July 2010
[7] Lansford, Jim; Stephens, A.; Nevo, R., "Wi-Fi (802.11b) and Bluetooth: enabling coexistence," *Network, IEEE* , vol.15, no.5, pp.20,27, Sep/Oct 2001
[8] Shuyan Jiang; Jie Peng; Zhi Lu; Junjie Jiao; Shanshan Jiang, "802.11ad Key Performance Analysis and Its Application in Home Wireless Entertainment," *Computational Science and Engineering (CSE), 2014 IEEE 17th International Conference on* , vol., no., pp.1595,1598, 19-21 Dec. 2014
[9] Haiyan Li, "Channel Capacity and Channel Estimation of OFDM Ultra-Wide-Band Systems," *Computer Science and Electronics Engineering (ICCSEE), 2012 International Conference on* , vol.2, no., pp.152,156, 23-25 March 2012
[10] Chavan, M.S; Chile, R.H; Sawant, S.R, "Multipath Fading Channel Modelling and Performance Comparision of Wireless Channel Models, " *International Journal of Electronics and Communication Engineering*, Vol. 4, no.2, pp. 189-203, 2011
[11] S. Ghassemzadeh, L. Greenstein, T. Sveinsson, A. Kavcic, and V. Tarokh, "Uwb indoor path loss model for residential and commercial environments, " in *IEEE VTC 2003- Fall*, 2003.
[12] A. Saleh and R. A. Valenzuela, "A statistical model for indoor multipath propagation," IEEE *J. Selected Areas Comm.*, vol. 5, pp. 138–137, Feb. 1987